Acta Biomaterialia 6 (2010) 2970–2978

Contents lists available at ScienceDirect

Acta Biomaterialia

journal homepage: www.elsevier.com/locate/actabiomat

# Varying the diameter of aligned electrospun fibers alters neurite outgrowth and Schwann cell migration

Han Bing Wang [a,b], Michael E. Mullins [b], Jared M. Cregg [a], Connor W. McCarthy [a], Ryan J. Gilbert [a,*]

[a] Regeneration and Repair Laboratory, Department of Biomedical Engineering, Michigan Technological University, Houghton, MI 49931-1295, USA
[b] Department of Chemical Engineering, Michigan Technological University, Houghton, MI 49931-1295, USA

ARTICLE INFO

*Article history:*
Received 11 August 2009
Received in revised form 6 January 2010
Accepted 10 February 2010
Available online 16 February 2010

*Keywords:*
Aligned fibers
Electrospinning
Poly-L-lactic acid
Nerve regeneration

ABSTRACT

Aligned, electrospun fibers have shown great promise in facilitating directed neurite outgrowth within cell and animal models. While electrospun fiber diameter does influence cellular behavior, it is not known how aligned, electrospun fiber scaffolds of differing diameter influence neurite outgrowth and Schwann cell (SC) migration. Thus, the goal of this study was to first create highly aligned, electrospun fiber scaffolds of varying diameter and then assess neurite and SC behavior from dorsal root ganglia (DRG) explants. Three groups of highly aligned, electrospun poly-L-lactic acid (PLLA) fibers were created (1325 + 383 nm, large diameter fibers; 759 + 179 nm, intermediate diameter fibers; and 293 + 65 nm, small diameter fibers). Embryonic stage nine (E9) chick DRG were cultured on fiber substrates for 5 days and then the explants were stained against neurofilament and S100. DAPI stain was used to assess SC migration. Neurite length and SC migration distance were determined. In general, the direction of neurite extension and SC migration were guided along the aligned fibers. On the small diameter fiber substrate, the neurite length was 42% and 36% shorter than those on the intermediate and large fiber substrates, respectively. Interestingly, SC migration did not correlate with that of neurite extension in all situations. SCs migrated equivalently with extending neurites in both the small and large diameter scaffolds, but lagged behind neurites on the intermediate diameter scaffolds. Thus, in some situations, topography alone is sufficient to guide neurites without the leading support of SCs. Scanning electron microscopy images show that neurites cover the fibers and do not reside exclusively between fibers. Further, at the interface between fibers and neurites, filopodial extensions grab and attach to nearby fibers as they extend down the fiber substrate. Overall, the results and observations suggest that fiber diameter is an important parameter to consider when constructing aligned, electrospun fibers for nerve regeneration applications.

Published by Elsevier Ltd.

## 1. Introduction

Electrospun fibers are being developed as tissue engineering scaffolds because their geometric scale is similar to protein fibers within the native extracellular matrix (ECM) [1–3]. Several factors make electrospun fibers an attractive scaffold for tissue engineering. The technique of producing electrospun fibers is relatively simple, cost-effective and flexible [3–5]. Many different varieties of polymers have been electrospun as cell scaffolds [6,7] or drug carriers [8,9]. Multiple types of electrospun fibers such as random [10,11], aligned [12–16], and hollow or porous structures [17,18] are capable of supporting the attachment and proliferation of a variety of cell types. Furthermore, the geometrical properties of the fiber (such as its diameter) can be controlled by changing the polymer solution parameters [19] and processing conditions [20–22].

Compared to a smooth surface or a scaffold with random structures, aligned structures are capable of guiding neurite extension through a lesion site for regeneration within the peripheral nervous system (PNS) or spinal cord [23–28]. Aligned, electrospun fibers and aligned filaments direct in vitro neurite extension [12–15,25,29,30]. However, it is difficult to maintain a uniform fiber diameter within electrospun fiber samples. For example, neurites from rat embryonic day 15 (E15) DRG proceeded along the aligned poly-L-lactide fiber scaffolds where the mean diameter was 524 nm but fiber diameter ranged from 150 to 1540 nm [12]. Most commonly, nanoscale, aligned, electrospun fibers are constructed to examine their ability to foster directed neurite outgrowth. For instance, aligned fibers with diameters in the nanoscale range (400–600 nm) constructed from acrylonitrile-co-methylacrylate guided neurite outgrowth from rat DRG [25]. Neurites from E10 chick dorsal root ganglia (DRG) also extended down nanofibers

* Corresponding author. Tel.: +1 906 487 1740; fax: +1 906 487 1717.
*E-mail address:* rgilbert@mtu.edu (R.J. Gilbert).

1742-7061/$ - see front matter Published by Elsevier Ltd.
doi:10.1016/j.actbio.2010.02.020

constructed of poly-ε-caprolactone (PCL) and collagen/poly-ε-caprolactone (C/PCL) [30]. In another recent study, neurites from E10 chick DRG were guided along aligned nanofibers made from PCL and were not guided when introduced to crossed patterns [15].

While electrospun nanofibers have been more extensively studied than fibers with diameters in the micron range, electrospun fibers or polymer filaments with diameters in the micron range also effectively direct neurite extension. Postnatal day 1 rat DRG neurite extension was more prolific on subcellular size filaments (5 μm) than on large diameter species [29]. Neurites from E9 chick DRG extended along aligned fibers whose diameter was between 1 and 2 μm [14]. From examination of these studies, it was clear that neurites emanating from DRG on aligned nanofibers extended longer neurites parallel to the aligned fibers. However, in some images, neurite extension perpendicular to the aligned, electrospun fibers was also seen [12,15,30]. Thus, it may be possible to alter topographical properties (e.g. fiber diameter) to minimize perpendicular neurite extension and promote more effective, longer neurite extension along the aligned substrate.

Our previous research has shown that highly aligned fibers with diameters in the 1–2 μm range have great potential in guiding in vitro neurite outgrowth from DRG explants in a directed manner [14]. We hypothesize that the surface morphology of aligned, electrospun fiber scaffolds such as fiber diameter is an important parameter that affects cell attachment, cell migration, and neurite orientation and extension from explants. The objective of this study was to create highly aligned fiber scaffolds with distinct differences in fiber diameter. Once the fiber scaffolds were fabricated and characterized, E9 chick dorsal root ganglia (DRG) were cultured on the fiber scaffolds to study how neurites interact with the fibers and to examine the effect of fiber diameter on neurite extension and Schwann cell (SC) migration. This study shows that the direction and extent of neurite extension and SC migration from DRG explants is influenced significantly by fiber diameter.

## 2. Materials and methods

### 2.1. Preparation of aligned, PLLA electrospun fibers with different diameters

Poly-L-lactic acid (PLLA) fibers were fabricated using an electrospinning setup described in our previous study [14]. Briefly, three fiber groups with different diameters were fabricated in this study. To obtain the large diameter (1325 ± 383 nm) fibers, 8 wt.% PLLA (NatureWorks™; grade 6201D, Cargill Dow LLC, Minnetonka, MN) was dissolved in a mixture of chloroform and dichloromethane (50:50 wt.%) (Sigma–Aldrich, St. Louis, MO) at room temperature. 8 wt.% PLLA was dissolved in 1,1,1,3,3,3-hexafluoro-2-propanol (HFP, Fluka/52512, Sigma–Aldrich) which yielded intermediate (759 ± 179 nm) diameter fibers. The addition of 0.2 wt.% of 10× phosphate-buffered saline (PBS) (Invitrogen, Carlsbad, CA) into a PLLA/HFP solution, created the small diameter fibers (293 ± 65 nm). All fibers were electrospun with a 22 G sharp-tip needle (Fisher Scientific, Hanover Park, IL). The tip of the needle was insulated with a piece of tubing so that the electrical force would concentrate on the needle tip, and consequently enhance the electrospinning efficiency. The syringe pump flow rate for all experiments was fixed at 2 ml $h^{-1}$, and the working voltage was held constant at 15 kV. The fibers were collected on 15 × 15 mm glass coverslips (Proscitech, Australia), attached on the edge of a rotating disk (220 mm in diameter with a thickness of 10 mm) using a piece of double-sided tape (3M; St. Paul, MN). 4 wt.% PLLA was used to make a thin layer of film to maintain fiber position and alignment. With this concentration, the viscosity of the polymer solution is suitable to cast the film. The mechanical properties of the film are appropriate for manipulation into three-dimensional scaffolds for use in other studies. PLLA was dissolved in a mixture of chloroform and dichloromethane (50:50 wt.%), and the solution was then cast on a coverslip prior to electrospinning. A thin layer of film formed as the solvent evaporated. Detailed working conditions of electrospinning and other parameters are shown in Table 1.

### 2.2. Cell culture

E9 chick DRG were isolated in accordance with procedures approved by the Institutional Animal Care and Use Committee (IACUC) at Michigan Technological University. Fiber samples were sterilized with an ethylene oxide sterilization system (Andersen Sterilizers Inc., Haw River, NC) for 12 h prior to culturing. DRG were isolated using previously published protocols [14]. Briefly, 200 μl of neurobasal media was placed on a fiber specimen. Then ganglia were divided into halves and placed within the neurobasal media droplet onto fibers. The culture experiments were repeated three times using independently fabricated fiber samples. DRG were allowed to attach onto fibers for approximately 6 h in a tissue culture incubator (37 °C, 5% $CO_2$) before adding another 1.8 ml of neurobasal media (with L-glutamine, penicillin/streptomycin and B-27 (Invitrogen), supplemented with 50 ng $ml^{-1}$ of nerve growth factor (NGF) (Calbiochem, La Jolla, CA)). The DRG were then incubated for 5 days, with media being exchanged every 60 h.

### 2.3. Immunocytochemistry

#### 2.3.1. Neurofilament stain

After 5 days of culture, DRG samples were fixed with 4% (w/v) paraformaldehyde (Sigma–Aldrich) in PBS (Invitrogen) solution for 30 min. Samples were washed three times with PBS, and then blocked with a solution containing 2% normal goat serum (Invitrogen), 2% non-fat dry milk (TVC Inc., Brevard, NC) and 0.05% Triton X-100 (EMD Chemicals, Gibbstown, NJ) for 30 min. After washing three times with PBS, samples were incubated (37 °C, 5% $CO_2$) with rabbit anti-neurofilament (145 kD intermediate neurofilament) primary antibody (1:200 dilution) (Millipore, Temecula, CA) for 1 h, and then washed three times with PBS. The specimens were incubated with an Alexa Fluor 488 goat anti-rabbit secondary antibody (Invitrogen) for another hour and washed three times with PBS.

#### 2.3.2. Schwann cell stain

DRG samples were fixed with 4% (w/v) paraformaldehyde for 1 h. Samples were washed three times with PBS, and then blocked with a solution containing 10% normal goat serum (Invitrogen), 2% bovine serum albumin (BSA, Sigma–Aldrich), 0.4% Triton X-100

**Table 1**
Electrospinning parameters for fabrication of aligned fibers with different diameters.

| Fiber type | Fiber diameter (nm ± standard deviation) | Collector speed (rpm) | Solvent | Espin time (min) | Working distance (cm) |
|---|---|---|---|---|---|
| Small diameter | 293 ± 65 | 3000 | 1,1,1,3,3,3-Hexafluoro-2-propanol (HFP) +0.2% 10× PBS | 3 | 3 |
| Intermediate diameter | 759 ± 179 | 1500 | 1,1,1,3,3,3-Hexafluoro-2-propanol (HFP) | 6 | 6 |
| Large diameter | 1325 ± 383 | 1500 | Chloroform/dichloromethane = 50/50 | 10 | 6 |

(Sigma–Aldrich) for another hour. Samples were then immunostained using rabbit anti-S100 primary antibody (1:200 dilution) (Dako, Denmark) at 4 °C overnight. Secondary antibody Alexa Fluor™ 488 goat anti-rabbit IgG (1:500 dilution, Invitrogen) was applied for 1 h at room temperature (RT). Samples were then washed three times with PBS.

4′, 6-diamidino-2-phenylindole dihydrochloride (DAPI, Sigma–Aldrich) was diluted to a final working concentration of 1 μg $ml^{-1}$. Two-hundred microliters of DAPI was added to the neurofilament-stained or S100-stained samples 5 min prior to imaging. DRG were imaged using a Zeiss Axiovert 200 M microscope equipped with an AxioCam camera.

### 2.4. Scanning electron microscopy (SEM) analysis of fiber and cell samples

SEM was conducted using a Hitachi S-4700 field emission scanning electron microscope at an accelerating voltage of 2 kV. All of the samples (fiber samples and cell samples) were coated with 5 nm of gold by a Hummer 6.2 sputter coater (Anatech Ltd., Denver, NC).

Plain fiber samples were coated with gold without any pretreatment. For cell samples, the samples were fixed with 4% (w/v) paraformaldehyde in 1× PBS buffer for 30 min, and then post-fixed with 1% osmium tetroxide (Sigma–Aldrich) in distilled water for 1 h. Samples were dehydrated with a series of graded ethanol washes (50/70/80/90/100% in water). Subsequently, the samples were immersed in hexamethyldisilizane (HMDS, Sigma–Aldrich) for 5 min, and then transferred to a desiccator for 30 min.

### 2.5. Characterization of fiber diameter, alignment and packing density

SEM images of the fibers were taken from three independently fabricated sample batches for each fiber condition. Fifty fibers from each SEM image were selected for diameter and alignment analysis. Thus, a total of 150 fibers were used to generate each graph. The diameter and alignment of fibers were characterized using methods described previously [14]. Packing density was measured to describe the spacing between the aligned fibers. Using SEM images of three areas within each sample, three independently fabricated samples were analyzed for each fiber condition ($n = 9$). Measurement of packing density utilized a method similar to neurite density measurement. The percentage of black pixels in the whole image indicates the fraction of fibers in the total area. A lower percentage of black pixels signifies that there is more space between fibers. For alignment analysis, a reference line was drawn along the fiber orientation. The angle between the line and each individual fiber was calculated and placed into a data bin of 2°. The angular difference ranged from 90° to −90° with 0° being parallel to the reference line. Fast Fourier transform (FFT) was also used to characterize the alignment of the fibers. The resulting FFT output image reflects the degree of fiber alignment. A square region of 2048 × 2048 pixels on the SEM image was randomly selected and processed by FFT using the National Institutes of Health (NIH) Image J software.

### 2.6. Length of neurite outgrowth

When the neurite outgrowth was longer than 1.5 times the DRG diameter, the DRG was considered viable [31]. Twelve viable DRG with DRG areas ranging between 0.25 and 0.4 $mm^2$ were selected for subsequent analysis for each fiber condition. The perimeter of each selected DRG was marked and the 10 longest neurites from one side of the DRG were measured and averaged to generate the average neurite length for that particular side of the DRG. The same analysis was then conducted on the other side of the DRG. Twelve DRG were analyzed on the large, intermediate and small diameter fiber samples. Since each DRG has two sides of neurite outgrowth, 24 length measurements ($n = 24$) were gathered for each fiber condition. All measurements were taken using NIH Image J software.

### 2.7. Degree of perpendicular neurite outgrowth

To determine how fiber diameter affected neurite extension perpendicular to the axis of the aligned fibers, the degree of perpendicular neurite outgrowth was quantified. The perimeter of each DRG characterized in Section 2.6 was marked using NIH Image J software. The distance from the top and the bottom of the explants to the maximum neurite extension that occurred perpendicular to the aligned fibers was measured as neurite perpendicular outgrowth ($n = 24$ for each fiber condition).

### 2.8. Schwann cell migration

The migration of SCs on fibers was characterized using DAPI nuclei stain. To compare the rate of SC migration and neurite extension, the same 12 DRG used for neurite length analysis were selected for migration distance measurement. As shown in Fig. 1, two rectangles were drawn from the edge of the DRG to the edge of the migrated SCs. The migration distance on both sides of the DRG was quantified as the distance across the rectangles (length) ($n = 24$ for each diameter condition).

### 2.9. Statistical analysis

Statistical analyses were performed using JMP IN software (release 5.1.2; SAS, Cary, NC). A one-way ANOVA was run first to determine statistical difference between groups in fiber diameters ($n = 150$), neurite length ($n = 24$), perpendicular neurite outgrowth ($n = 24$), Schwann cell migration distance ($n = 24$) and fiber packing density ($n = 9$). For the groups that showed differences in ANOVA, post hoc Tukey–Kramer HSD tests were used to compare all pairs individually. The Brown–Forsythe test was run to determine statistical differences in fiber alignment ($n = 150$). A value of $P < 0.05$ was considered to be statistically significant.

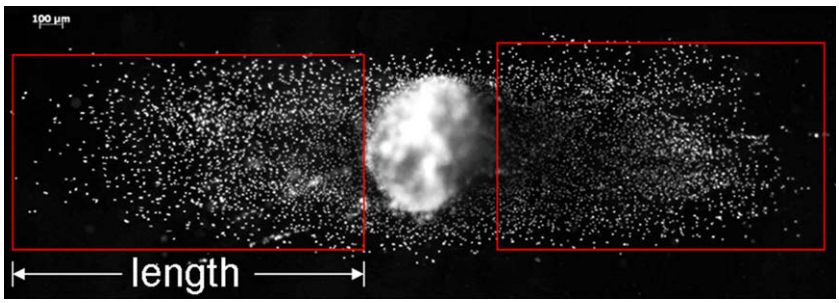


**Fig. 1.** Schematic of SC migration distance measurement. The distance was measured as the length of the rectangle.

## 3. Results

### 3.1. Morphology of the fibers

The morphology of the fibers was observed using a field emission scanning electron microscope. Diameter, alignment of the fibers and the packing density were characterized using NIH Image J software. In Fig. 2, fiber diameters varied when electrospinning was conducted with different solvents and a small amount of PBS. Fig. 2A–C shows an SEM image (A), a FFT output image (B), and the angular difference measurements (C) of large diameter fibers. Fig. 2D–F presents the corresponding images for intermediate diameter fibers, and Fig. 2G–I are those for small diameter fibers. FFT images were taken from 2048 × 2048 pixel selections of the original SEM images, which generated an output image containing pixels with a symmetrical shape. The narrower area of the center parts in FFT output images indicates better fiber alignment. Fig. 2 demonstrates that large diameter and intermediate diameter fibers

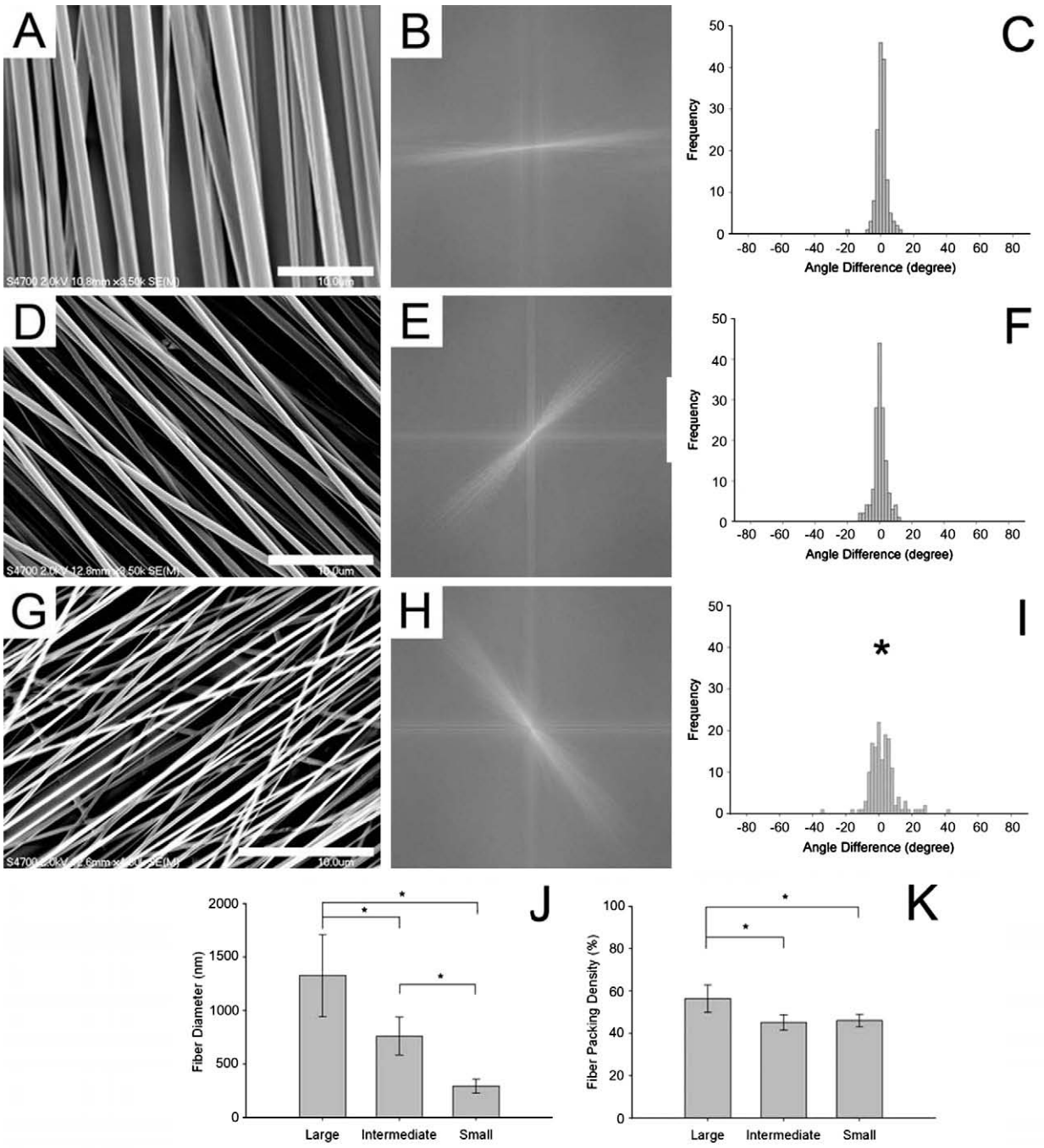


**Fig. 2.** Alignment and diameter of PLLA fibers. (A) SEM images of fibers with a large diameter, 1325 ± 383 nm; (B) FFT images from a 2048 × 2048 pixel selection from image (A); (C) histograms of angular difference showing the alignment of large diameter fibers. (D–F) SEM image, FFT image and angular difference showing the alignment of intermediate diameter fibers, 759 ± 179 nm. (G–I) SEM image, FFT image and angular difference showing the alignment of small diameter fibers, 293 ± 65 nm. In FFT images, the center area depicts the alignment of the fibers. The narrower areas represent better alignment. For angular difference images, the sharper peak indicates more fibers are parallel to each other, which means better alignment. The alignment of large fibers (C) and intermediate fibers (F) is statistically different (better) from that of small fibers (I) (*$P < 0.05$). (J) Graph of the fiber diameters. (K) Graph of fiber packing density (*$P < 0.05$). Scale bar = 10 μm. Error bars indicate ± standard deviation (SD).

were highly aligned. The alignment of small diameter fibers was statistically different (*$P < 0.05$). However, as shown in Fig. 2I, the small diameter fiber samples are still very highly aligned. Eighty-eight percent of the small diameter fibers were varied within +10°. Fig. 2J reveals that there is a statistically significant difference in fiber diameter between each fiber pair. The average fiber diameter was 1325 ± 383 nm for the large diameter samples, 759 ± 179 nm for the intermediate diameter fibers and 293 ± 65 nm for small diameter fibers (mean + SD). Fig. 2K depicts the pixel fraction of fibers in the whole image. A larger fraction indicates more densely packed fibers. As shown in Fig. 2K, large diameter fibers have a statistically significant higher packing density than intermediate and small diameter fibers. For intermediate and smaller fibers, the packing density is 45% and 46%, respectively, which is about 9% lower than the large diameter fibers.

### 3.2. Neurite extension on different diameter fiber scaffolds

E9 chick DRG were cultured on fiber substrates of varying diameters to investigate how fiber diameter affected neurite extension that was either parallel or perpendicular to the aligned fibers. Neurofilament-stained images from DRG cultured on large diameter fibers, intermediate diameter fibers and small diameter fiber samples are shown in Fig. 3A–C, respectively. When determining which scaffolds promoted the longest neurite extension, DRG on the large and intermediate fibers produced significantly longer neurites than those seen in the small diameter fiber samples (Fig. 3D). In an attempt to quantify how fibers restrict neurites growing across the fibers, the extent of perpendicular neurite outgrowth was determined (Fig. 3E). The results show that DRG cultured on the small diameter fiber scaffolds had the longest

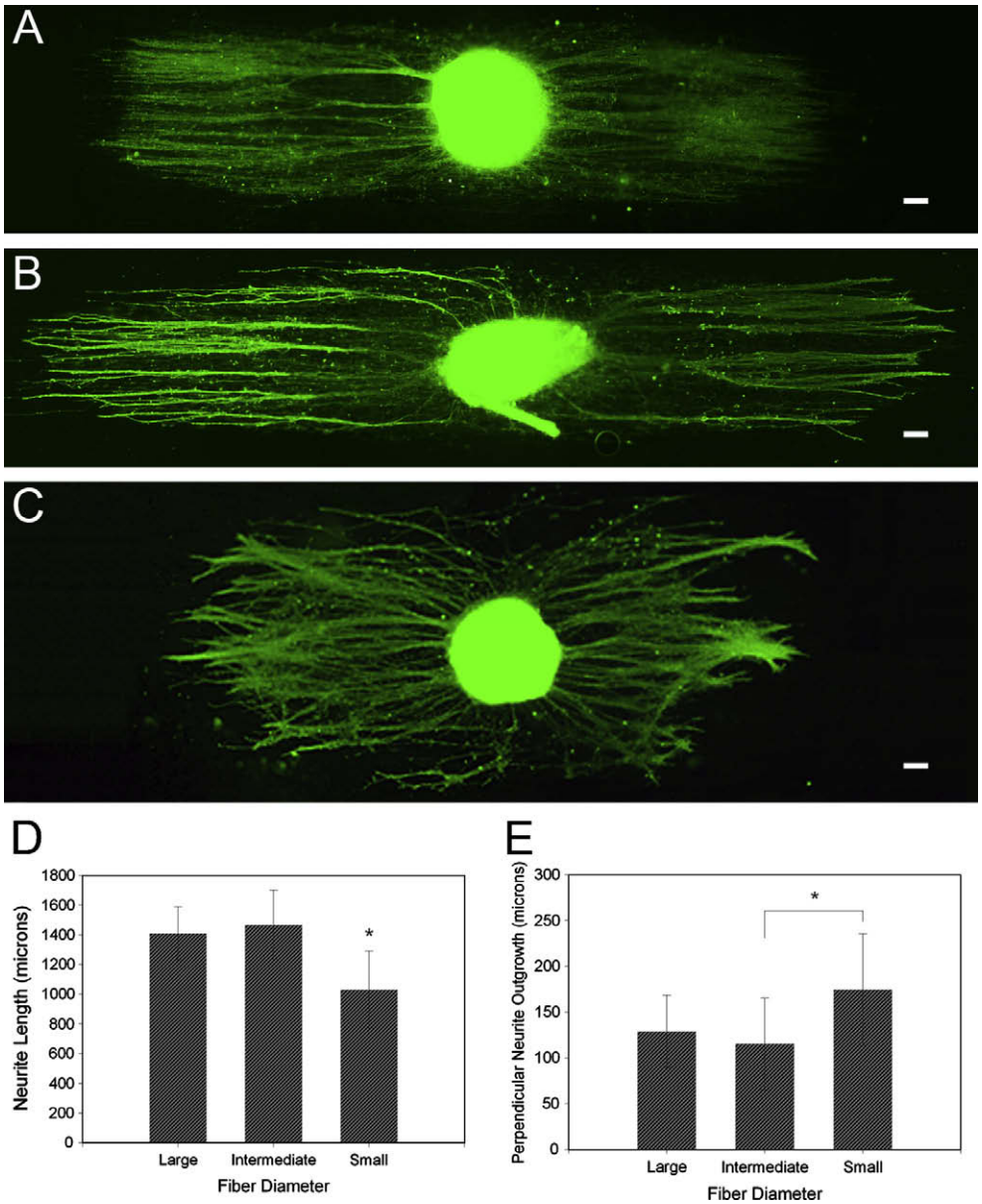


**Fig. 3.** Effect of fiber diameter on neurite outgrowth in parallel and perpendicular directions to the fibers. (A) Neurofilament-stained image of DRG cultured for 5 days on large diameter fibers. (B) Neurofilament-stained DRG cultured on intermediate diameter fibers. (C) Neurofilament-stained DRG on small diameter fibers. (D) Neurite length parallel to the fiber direction for each fiber condition (large, intermediate, small) indicates that neurites grown on small fibers were statistically shorter (*$P < 0.05$). (E) Perpendicular neurite outgrowth on each fiber condition reveals that on small diameter fibers, neurites crossed the fibers and grew longer in the perpendicular direction (*$P < 0.05$). Scale bar = 100 μm. Error bars indicate ± standard deviation (SD).

perpendicular outgrowth, and there was only a significant difference between the small and intermediate diameter samples ($^*P < 0.05$).

### 3.3. Schwann cell migration on different diameter fiber scaffolds

SCs migrating from DRG were characterized using a DAPI nuclei stain for two reasons. First, as shown in Fig. 4B–D, S100/DAPI double-stained images indicate that DAPI-stained cells were the nuclei of SCs. Second, DAPI-stained images more clearly show the position of SCs because DAPI stains cell nuclei. Within S100-stained images, it is difficult to distinguish SCs from neurites if the SCs overlap or are in close proximity to neurites (as shown by the red arrow in Fig. 4A). The S100 antibody occasionally can label SCs and neurites within the same sample and this has appeared in other studies [25,30].

Fig. 5A–F shows DAPI-stained images and neurofilament/DAPI double-stained images of DRG cultured for 5 days on large diameter (A, B), intermediate diameter (C, D) and small diameter fibers (E, F). Fig. 5G indicates that SC migration away from DRG explants was furthest on large diameter fiber samples, and shortest on small diameter fiber samples. All groups were statistically different ($^*P < 0.05$). Fig. 5H shows that the extent of SC migration did not always correlate with the extent of neurite extension. On intermediate fiber scaffolds, SC migration lagged behind neurite extension ($^*P < 0.05$), while on large diameter fibers and small diameter fibers, SC migration occurred at the same rate as neurite extension.

### 3.4. Neurite interaction with fibers

SEM analysis was conducted after DRG were cultured for 5 days. SEM images were captured at the leading edge of neurite extension to reveal how the neurites utilize the fibers to facilitate directed neurite extension (Fig. 6A–C). At the leading edge of neurite extension, neurites attached to the fiber surface instead of extending between fibers. Additionally, at the neurite/fiber interface, filopodia extended that traversed over several adjacent fibers. This was observed in all the fiber samples.

## 4. Discussion

Aligned, electrospun fibers effectively direct neurite extension from primary cell explants [12,14,15,25,30] and within sciatic nerve injury models [25,28]. From these previous studies, most of the aligned, electrospun fibers had diameters in the nanometer range. While analyzing in vitro neurite outgrowth within these studies [12,15,30], neurite outgrowth was along the fiber direction, but some outgrowth also occurred perpendicular to the orientation of the fibers. It is unknown how specific electrospun fiber diameters within an aligned scaffold influence the degree and the direction of neurite outgrowth from primary cell explants culture. Using different solvents and a small amount of ionic solution (PBS) as an additive, and by manipulation of the electrospinning parameters (disk rotation speed and collecting distance), three distinct fiber scaffolds with unique diameters were created. As described elsewhere, the fibers constructed for this study effectively directed neurite extension and SC migration without requiring a pre-coat of cell adhesive proteins/peptides [12,14,30]. From the data presented here, neurite outgrowth along the fibers was more directed and longer on the large and intermediate diameter fibers. The mean perpendicular distance of neurites on the small diameter fibers was significantly longer when comparing that of intermediate diameter fibers, which means that neurites crossed more fibers on the small diameter fiber scaffolds.

From our observations, SC migration patterns were also influenced by fiber diameter and did not always correlate with neurite

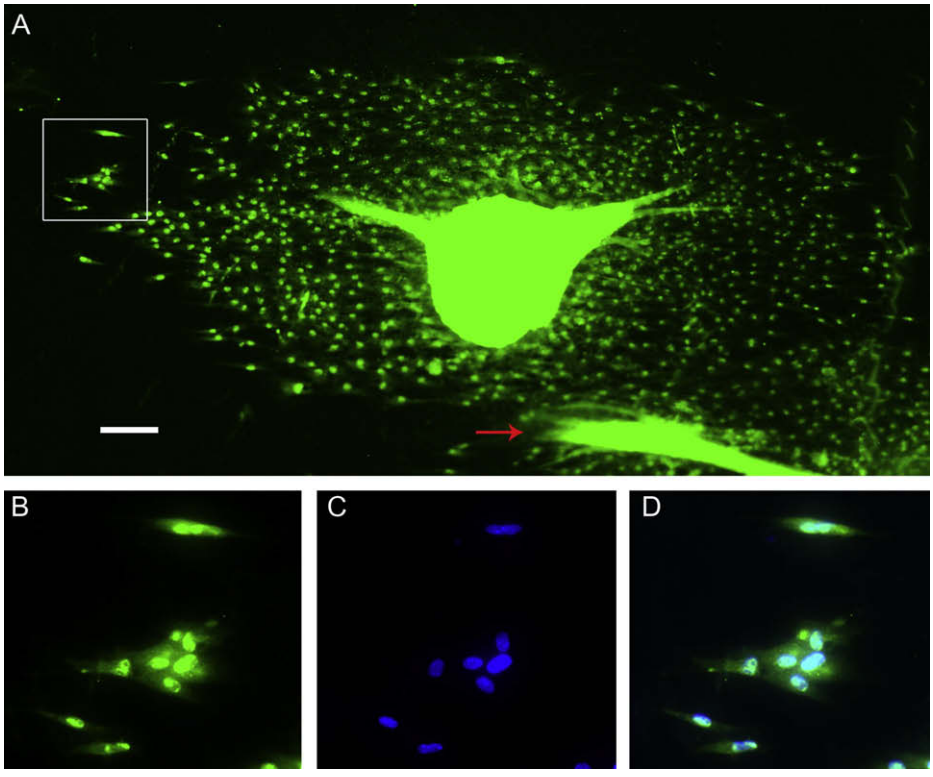


**Fig. 4.** SC migration from DRG explants. (A) Overview of S100-stained SCs after 5 days of culture. Red arrow indicates neurite extension from a nearby DRG. The square area in (A) is enlarged as (B–D). (B) S100-stained SC; (C) DAPI-stained SC nuclei; (D) combined image of (B) and (C), which indicates that DAPI-stained SC match the position of S100-stained SCs. Quantification of SC migration using DAPI staining matches the position of SCs. Scale bar = 100 μm.

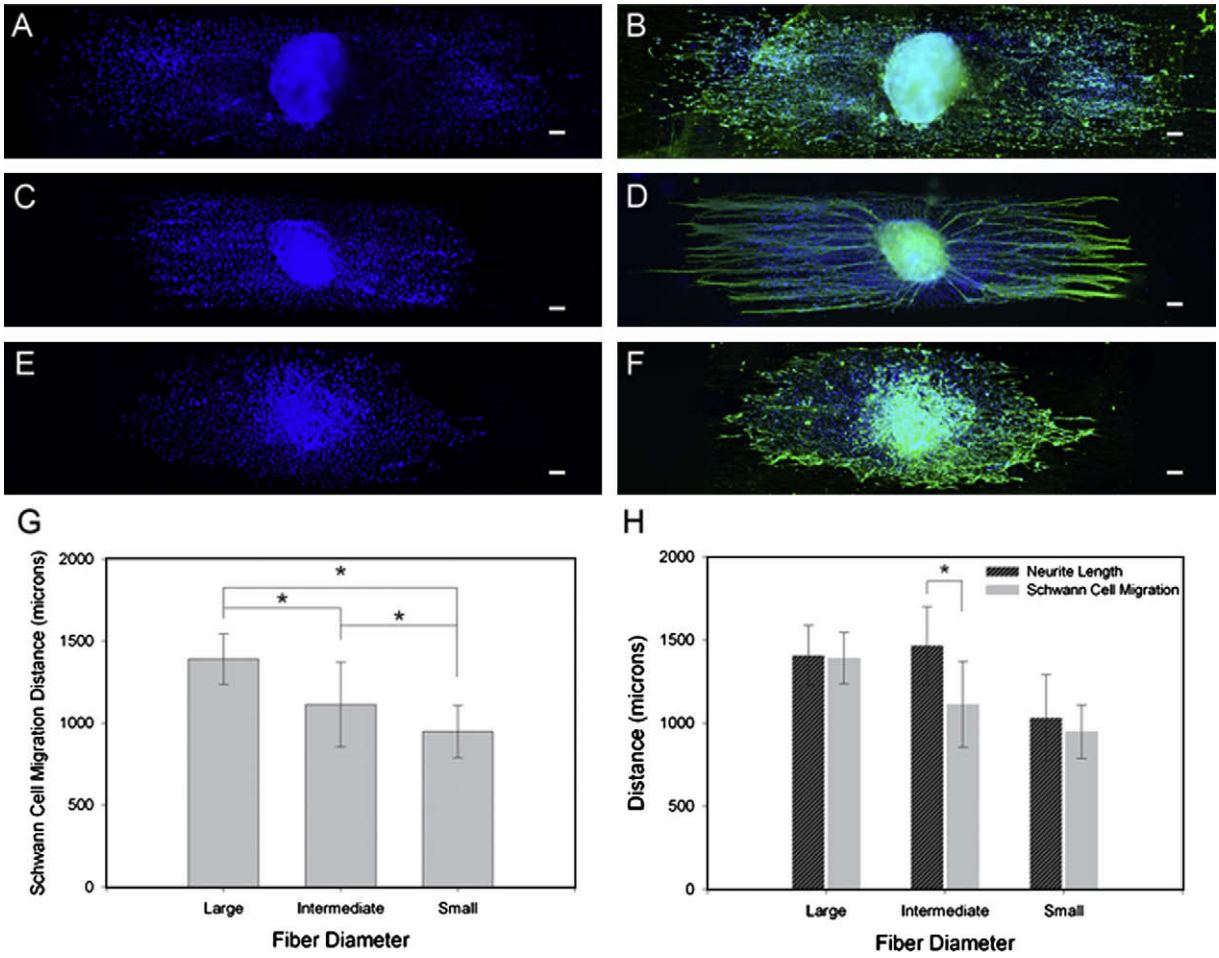


**Fig. 5.** Effect of fiber diameter on SC migration. (A) DAPI-stained images showing SC migration on large fibers. (B) Neurofilament/DAPI-combined images showing DRG cultured for 5 days on large diameter fibers. (C and D) DAPI-stained SCs and neurofilament/DAPI-combined images of DRG cultured on intermediate diameter fibers. (E and F) DAPI-stained and neurofilament/DAPI-combined images of DRG cultured on small diameter fibers. (G) Quantitative analysis shows that SC migration was greatest on the large fibers, and shortest on small fibers (*$P < 0.05$). (H) Graph shows the relationship of neurite outgrowth and SC migration along the fiber orientation. On intermediate diameter fiber scaffolds, neurite length was statistically greater than SC migration distance (*$P < 0.05$). Scale bar = 100 μm. Error bars indicate ± standard deviation (SD).

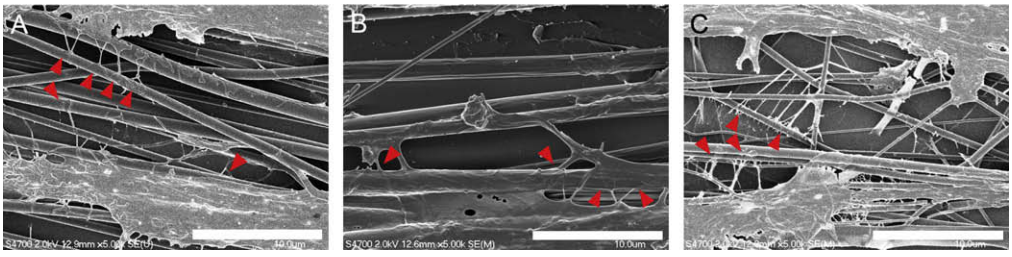


**Fig. 6.** SEM images of DRG cultured on fiber scaffolds with different diameters: (A) neurites on large diameter fibers; (B) neurites on intermediate diameter fibers; and (C) neurites on small diameter fibers. Neurites spread over the surface of the fiber instead of existing between fibers. Small filopodia (red arrows) were observed emanating from the neurites on each fiber condition. Scale bar = 10 μm.

extension. SCs lagged behind neurites grown on intermediate diameter fiber scaffolds, but grew to the same extent as neurites on the large and small diameter scaffolds. In previously published studies, it was observed that SCs migrate first, then neurites follow, and the neurites extend out on top of the SCs [25,30]. This type of behavior was shown by the small and large diameter species presented here. In the case of the small diameter fibers, the inability to create highly aligned fibers may have resulted in diminished neurite and SC migration. Because neurites and SCs are much larger than the small diameter fibers, they may have a more difficult time detecting individual fibers and deciding which groups of fibers to migrate along. The small diameter fibers also may pose less of a barrier and that may be why perpendicular outgrowth and migration was observed. In one other study, axons were not guided by structures that were 100 nm in magnitude [32]. HFP was used as the solvent to fabricate intermediate and small diameter fibers. Additionally, a very small amount of PBS was added to the HFP when making small diameter fibers. The HFP solvent residue or salt content within the fibers may affect SC migration. However, to minimize solvent residue interference, samples were vented after preparation and kept in vacuo before sterilization. The amount of PBS added to the electrospinning solvent was low (10 μl PBS

solution per 5 g of electrospinning solvent). The solvent solution was used to fabricate approximately 15 fiber mats. Therefore, the amount of PBS salts released from the small diameter fiber samples was small and should not appreciably shift the osmotic potential of the culture media.

On the intermediate diameter fiber scaffolds, neurite outgrowth was directed along the fibers and SCs lagged behind neurites. The geometrical combination of alignment and diameter within intermediate diameter fiber samples may be very favorable for rapid growth of neurites along the aligned fibers. These rapidly extending neurites on the intermediate fiber samples may cover up topographical paths for SCs. Fig. 2K reveals there is more space between the intermediate fibers than the large diameter fibers. The intermediate diameter fibers that SCs can sense or attach to may be too far apart to facilitate strong SC migration.

Due to the difficulty in creating aligned, electrospun fibers of varying diameter, the effect of fiber diameter on neurite outgrowth and SC migration from primary cell explants had not previously been studied. From the results presented here, it is clear that fiber diameter influences the degree of cellular migration and extension. From previous studies, fiber diameter influenced neurite extension, cellular differentiation and migration of neural stem/progenitor cells on aligned [16] and randomly electrospun fiber samples [33]. Individual neural stem cells had longer neurites on the small diameter aligned fibers (average diameter 300 nm) compared to the larger diameter aligned fiber samples (average diameter 1.5 μm) [16]. Smaller diameter, randomly orientated fibers (283 ± 45 nm) facilitated more glial differentiation, while larger diameter randomly oriented fibers (749 ± 153 nm) facilitated more neuronal differentiation than cells cultured on tissue culture polystyrene in the presence of differentiating chemical agents. Small diameter fibers were also more likely to facilitate cell adhesion and enhance viability than the large fiber samples [35]. In this study, it was observed that DRG adhered more strongly to the large diameter scaffolds. This is not unexpected since these scaffolds facilitated the greatest amount of SC migration and neurite outgrowth.

From analysis of fiber packing density, the spacing between fibers is another parameter that may affect both neurite extension and SC migration. With large diameter fiber samples, fibers were more densely packed than with intermediate and small diameter fibers. These densely packed fibers not only act as a guidance cue to direct neurite extension and SC migration, but also act as a barrier to impede neurites and SCs from crossing onto nearby fibers. It is believed that this combination of fiber diameter and packing density displayed within the large diameter fiber samples is the reason why the most extensive and directed neurite outgrowth and SC migration occurred on the large diameter fiber samples. With intermediate diameter fibers, the alignment and diameter may be sufficient for neurite extension along the fibers. However, a larger spacing between fibers (10% larger than those in large fibers) may not provide enough topographical cues for prolific, directed SC migration. For DRG growth on small diameter fibers, the lack of a significant barrier (small fiber diameter) could allow cells and neurites to migrate onto nearby fibers. Reduced fiber alignment and lower fiber packing displayed within the small diameter fiber samples may also contribute to the less directed and less extensive neurite outgrowth and SC migration.

While stem cells have great promise in facilitating repair of the damaged nervous system, primary neurons and glia adjacent to the injury site must also interact favorably with and migrate through an electrospun fiber scaffold to enable functional recovery. Since there were no prior studies analyzing how electrospun fiber diameter influenced SC migration and neurite extension from primary cell explants, this study investigated the influence of fiber diameter on primary cell behavior. A comparison of the results presented here with results from neural stem cell studies suggests that when individual cells are placed onto aligned fiber substrates (dissociated neural stem cell studies), small fiber diameters (in the low nanometer range) may enable stronger attachment than their larger diameter counterparts and facilitate longer neurite outgrowth because of this greater initial cell attachment. The stronger attachment of these individual cells on small diameter species is probably due to there being more fibers within a particular area (greater surface area). In those situations in which the cells already have an established ECM, such as within a DRG explant, cells in the explant do not require greater surface areas to facilitate attachment. Extension or migration of cells out of the explant may allow cells to focus their energies on extension and/or migration rather than on attachment. Thus particular diameter and packing densities may be more favorable for individual cellular attachment vs. cell extension/migration if attachment is already available to the cell (such as within an explant). Whatever the specific reasons for the differences in outgrowth seen within this study, aligned fiber diameter influences cellular migration and extension from DRG explants. Future studies will attempt to assess how fiber diameter affects nerve regeneration outcomes within in vivo nerve regeneration models. In the design of these scaffolds for in vivo use, it is hypothesized that if strong directed SC migration into a scaffold containing aligned, electrospun fibers is desired (as is the case for peripheral nerve regeneration), large diameter aligned fiber scaffolds with a sufficient packing density may facilitate more robust regeneration outcomes than if using scaffolds with smaller diameter fibers. It is hypothesized that if strong neurite extension is desired with diminished glial migration (for possibly restricting the entry of glial scar producing cells within the spinal cord), intermediate fibers with a slightly lower packing density than the large diameter fiber samples may be considered. If a strategy employs the use of stem cells, then inclusion of small diameter fibers may be desirable to facilitate their adhesion to the scaffold before insertion into the injury site. Whatever the application may be, it is clear that electrospun fiber diameter and packing density within an aligned fiber scaffold should be carefully considered before designing scaffolds for nerve repair.

## 5. Conclusion

Aligned, electrospun fibers have significant potential to direct neurite outgrowth and are promising for nerve regeneration applications. However, careful attention to selecting certain geometrical parameters such as fiber alignment, diameter and density may assist in developing translational analogs that most efficiently direct and promote nerve regeneration. In this study, aligned fibers of different diameters were secured using a polymer film and neurite outgrowth and SC migration from chick DRG was characterized on aligned fiber scaffolds. The results here suggest that fiber diameter does influence neurite outgrowth and SC migration from the explant. Small diameter fibers (293 ± 65 nm) did not promote extensive neurite extension or SC migration. Intermediate diameter fibers (759 ± 179 nm) promoted long, directed neurite extension independent of SC migration, and large diameter fibers (1325 ± 383 nm) promoted long, directed neurite extension and SC migration. The packing density of fibers may also influence neurite extension and SC migration. Therefore, fiber diameter and the space between fibers should be carefully considered when constructing aligned, electrospun fiber constructs for nerve regeneration applications.

## Acknowledgements

This study was supported by the Department of Energy, USA, Research Excellence Fund Seed and Infrastructure Enhancement

Grants from Michigan Technological University, Michigan Technological University Summer Undergraduate Research Fellowship (SURF) and Michigan Space Grant Consortium (MSGC) (J.M.C.).

## Appendix A. Figures with essential colour discrimination

Certain figures in this article, particularly Figures 1–6, are difficult to interpret in black and white. The full colour images can be found in the on-line version, at doi: 10.1016/j.actbio.2010.02.020.

## References

[1] Pham QP, Sharmu U, Mikos AG. Electrospinning of polymeric nanofibers for tissue engineering applications: a review. Tissue Eng 2006;12:1197–211.
[2] Chew SY, Wen J, Yim EK, Leong KW. Sustained release of proteins from electrospun biodegradable fibers. Biomacromolecules 2005;6:2017–24.
[3] Sill TJ, von Recum HA. Electrospinning: applications in drug delivery and tissue engineering. Biomaterials 2008;29:1989–2006.
[4] Teo WE, Ramakrishna S. A review on electrospinning design and nanofibre assemblies. Nanotechnology 2006;17:R89–R106.
[5] Huang ZM, Zhang YZ, Kotaki M, Ramakrishna S. A review on polymer nanofibers by electrospinning and their applications in nanocomposites. Compos Sci Technol 2003;63:2223–53.
[6] Xu CY, Inai R, Kotaki M, Ramakrishna S. Aligned biodegradable nanofibrous structure: a potential scaffold for blood vessel engineering. Biomaterials 2004;25:877–86.
[7] Wan Y, Cao X, Zhang S, Wang S, Wu Q. Fibrous poly(chitosan-g-DL-lactic acid) scaffolds prepared via electro-wet-spinning. Acta Biomater 2008;4:876–86.
[8] Zeng J, Xu X, Chen X, Liang Q, Bian X, Yang L, et al. Biodegradable electrospun fibers for drug delivery. J Control Release 2003;92:227–31.
[9] Qi H, Hu P, Xu J, Wang A. Encapsulation of drug reservoirs in fibers by emulsion electrospinning: morphology characterization and preliminary release assessment. Biomacromolecules 2006;7:2327–30.
[10] Vaz CM, van Tuijl S, Bouten CV, Baaijens FP. Design of scaffolds for blood vessel tissue engineering using a multi-layering electrospinning technique. Acta Biomater 2005;1:575–82.
[11] Rho KS, Jeong L, Lee G, Seo BM, Park YJ, Hong SD, et al. Electrospinning of collagen nanofibers: effects on the behavior of normal human keratinocytes and early-stage wound healing. Biomaterials 2006;27:1452–61.
[12] Corey JM, Lin DY, Mycek KB, Chen Q, Samuel S, Feldman EL, et al. Aligned electrospun nanofibers specify the direction of dorsal root ganglia neurite growth. J Biomed Mater Res A 2007;83:636–45.
[13] Corey JM, Gertz CC, Wang BS, Birrell LK, Johnson SL, Martin DC, et al. The design of electrospun PLLA nanofiber scaffolds compatible with serum-free growth of primary motor and sensory neurons. Acta Biomater 2008;4:863–75.
[14] Wang HB, Mullins ME, Cregg JM, Hurtado A, Oudega M, Trombley MT, et al. Creation of highly aligned electrospun poly-L-lactic acid fibers for nerve regeneration applications. J Neural Eng 2009;6:016001.
[15] Xie J, MacEwan MR, Li X, Sakiyama-Elbert SE, Xia Y. Neurite outgrowth on nanofiber scaffolds with different orders, structures, and surface properties. ACS Nano 2009;3:1151–9.
[16] Yang F, Murugan R, Wang S, Ramakrishna S. Electrospinning of nano/micro scale poly(L-lactic acid) aligned fibers and their potential in neural tissue engineering. Biomaterials 2005;26:2603–10.
[17] Li D, Xia YN. Direct fabrication of composite and ceramic hollow nanofibers by electrospinning. Nano Lett 2004;4:933–8.
[18] McCann JT, Li D, Xia YN. Electrospinning of nanofibers with core-sheath, hollow, or porous structures. J Mater Chem 2005;15:735–8.
[19] Zhang C, Yuan X, Wu L, Han Y, Sheng J. Study on morphology of electrospun poly(vinyl alcohol) mats. Eur Polym J 2005;41:423–32.
[20] Deitzel J, Kleinmeyer J, Harris D, Beck Tan N. The effect of processing variables on the morphology of electrospun nanofibers and textiles. Polymer 2001;42:261–72.
[21] Zong XH, Kim K, Fang DF, Ran SF, Hsaio BS, Chu B. Structure and process relationship of electrospun bioabsorbable nanofiber membranes. Polymer 2002;43:4403–12.
[22] Subbiah T, Bhat GS, Tock RW, Parameswaran S, Ramkumar SS. Electrospinning of nanofibers. J Appl Polym Sci 2005;96:557–69.
[23] Cai J, Peng X, Nelson KD, Eberhart R, Smith GM. Permeable guidance channels containing microfilament scaffolds enhance axon growth and maturation. J Biomed Mater Res A 2005;75:374–86.
[24] Chew SY, Mi R, Hoke A, Leong KW. Aligned protein–polymer composite fibers enhance nerve regeneration: a potential tissue-engineering platform. Adv Funct Mater 2007;17:1288–96.
[25] Kim YT, Haftel VK, Kumar S, Bellamkonda RV. The role of aligned polymer fiber-based constructs in the bridging of long peripheral nerve gaps. Biomaterials 2008;29:3117–27.
[26] Yoshii S, Ito S, Shima M, Taniguchi A, Akagi M. Functional restoration of rabbit spinal cord using collagen-filament scaffold. J Tissue Eng Regen Med 2009;3:19–25.
[27] Ngo TT, Waggoner PJ, Romero AA, Nelson KD, Eberhard RC, Smith GM. Poly(L-lactide) microfilaments enhance peripheral nerve regeneration across extended nerve lesions. J Neurosci Res 2003;72:227–38.
[28] Clements IP, Kim YT, English AW, Lu X, Chung A, Bellamkonda RV. Thin-film enhanced nerve guidance channels for peripheral nerve repair. Biomaterials 2009;23–24:3834–46.
[29] Wen X, Tresco PA. Effect of filament diameter and extracellular matrix molecule precoating on neurite outgrowth and Schwann cell behavior on multifilament entubulation bridging device in vitro. J Biomed Mater Res A 2006;76:626–37.
[30] Schnell E, Klinkhammer K, Balzer S, Brook G, Klee D, Dalton P, et al. Guidance of glial cell migration and axonal growth on electrospun nanofibers of poly-epsilon-caprolactone and a collagen/poly-epsilon-caprolactone blend. Biomaterials 2007;28:3012–25.
[31] Kim IA, Park SA, Kim YJ, Kim SH, Shin HJ, Lee YJ, et al. Effects of mechanical stimuli and microfiber-based substrate on neurite outgrowth and guidance. J Biosci Bioeng 2006;101:120–6.
[32] Johansson F, Carlberg P, Danielsen N, Montelius L, Kanje M. Axonal outgrowth on nano-imprinted patterns. Biomaterials 2006;27:1251–8.
[33] Christopherson GT, Song H, Mao HQ. The influence of fiber diameter of electrospun substrates on neural stem cell differentiation and proliferation. Biomaterials 2009;30:556–64.